A

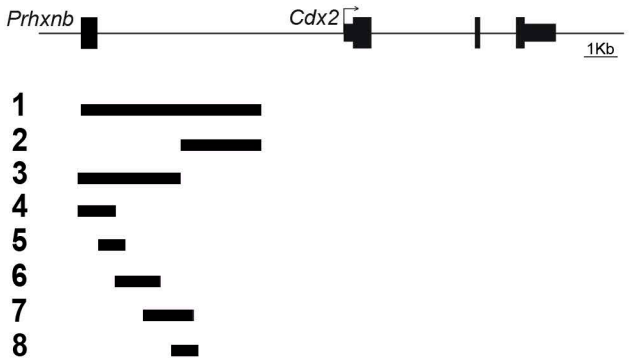

fragment	TE specificity	% reporter expressing
#1	+	47.00%
#2	-	2.27%
#3	+	25.42%
#4	-	6.98%
#5	-	11.11%
#6	+	21.75%
#7	-	4.00%
#8	-	9.26%

B

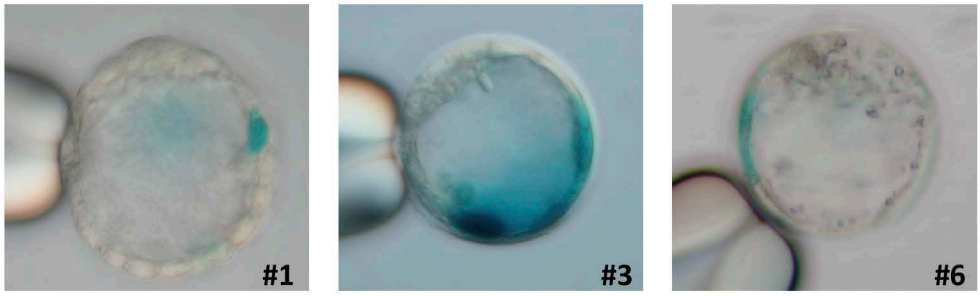

C

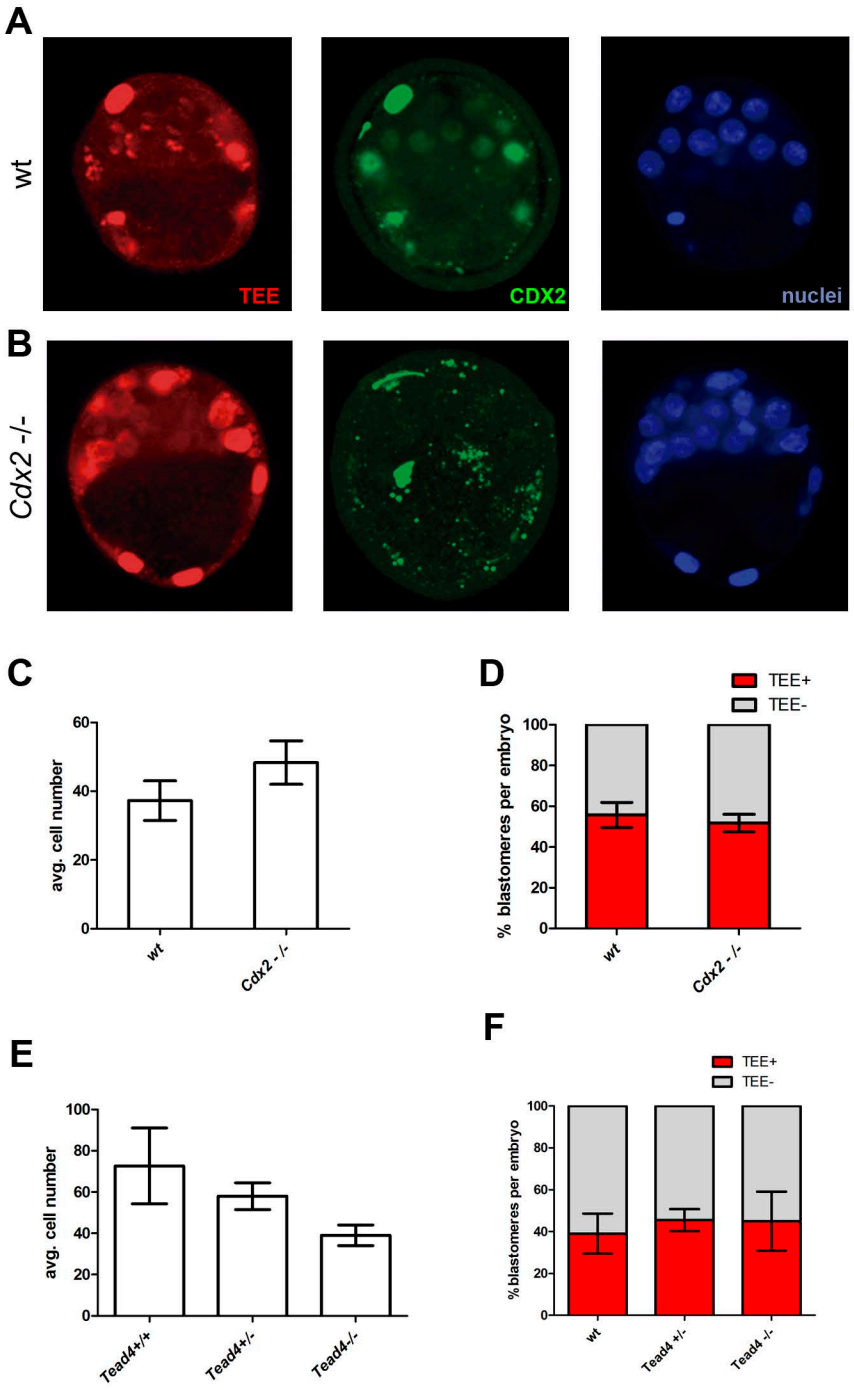
A
wt
TEE
CDX2
nuclei
B
Cdx2 -/-
C
avg. cell number
60
40
20
0
wt
Cdx2 -/-
D
TEE+
TEE-
% blastomeres per embryo
100
80
60
40
20
0
wt
Cdx2 -/-
E
avg. cell number
100
80
60
40
20
0
Tead4+/+
Tead4+/-
Tead4-/-
F
TEE+
TEE-
%blastomeres per embryo
100
80
60
40
20
0
wt
Tead4 +/-
Tead4 -/-

RayonS2

A

GAGCTCCACCGCGGTGGCGGCCGCGGGAATTCGATTCACACGGATGAATTGTCTGGTTTCCTAC
TGTAGTCAAAACACCTTATCCTCAAATTAGACTGTCTGGTTCTTTTTCATTTTCAATCTTTTAT
TTTTTTCTTGACG**AATTCCTA**AGTCACATATTAATTG**TTCCCACCG**AACGCAAAACAGCTATCC
TTGCGTCCTCCTGGAGTTTTCTGGGCCACAGGAGCGGTGCCTGCAGCGCAGTCTGGTCTCCCGC
ATGCTGCGCAGCAGAGGAGAAGAAACAAGGACCAGCGCCAGGCACAGGCTTGTCACTGTTAGAG
CCCAGATACGGAGGAAGGAAACTACCGACCATCCCTCCGCAACATGGGTCACCTGCCAG**TGTGG**
GAAACCGGCCTCTGCTACTTGGCTCCCTAGAAAGGGGTCTGAGTTGCCGGAAACCCGTCT**TTCC**
CAGGTCCCGGATGGCATCCAGCATTGCGCATCCTGCGCTGGCCTTCGGGCTACCAGCACTCCAG
CGTCTTTGGAAGAGTCCATGAGTAGCCCACTCCTGTCCCCTGGTCCCCCACCCCACCCACCCAAG
ACGCCAGGTGCCCAACCGGTGCCCTATCTCGGAGGGATAAGCTCTCAAGTGTTGAAATGCAGTT
ATGTCGCTGGATAGACCGGGTTGTTCCAGAGAGGCACAGGTTACATCTAGAATTGTAAAAATAG
CCCTGGAAATCGTGTCTCCTTGGATTCTCTGCATTGCTGGCTTAGCAAATTTACATAAAGAGGG
TGGATTCGGCATTTTAGAGCCTGGTTATCTAAGGGTTGGGTTTATCCCAAGGCTAGACAGAATG
CTTTGAATTATAGTGGGTGATTTTGAGTGTCTGTTTTGAGTGTGTGTTTTGAGTGGTGTGTGTG
TGTGTGTGTGTGTGTGTGTGTGTGTGTGTGTGTAAAAGAGAATGGGAGACACACAGAGAG
GAGACACAGGGGGGTGGGGGCAGGGAGCAGGGCCAAGCAGGGCTGGCATCCTCGAGCACCTGGT
GTCCTTCTTTCCTGCATGGCTCAGGCCTAGGATGCTGACTGAGGACTGGCAGCTTCCAAGGCAT
CCTTTCCCGCA**TTCCCACTT**TGTTCTCACTGCTCAGGGACGTAGGTGAGGTGACAGAAGAGCCA
ACAGGCAACTTTACTTCGATTCTGAGT**ATTCCAG**GAGGGGATTAGGTCTGTGGACCATCATGCA
TGTTCAGAGCCCAAAAGCTGTGGCACAGCTCTTTATGGAAAGGGAAAGAGGGTGGTTTTTTGTT

TEAD Site

RBPJ Site

B

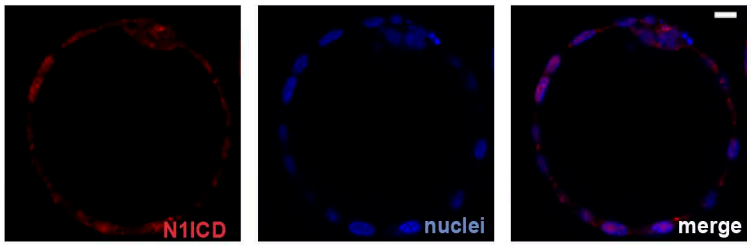

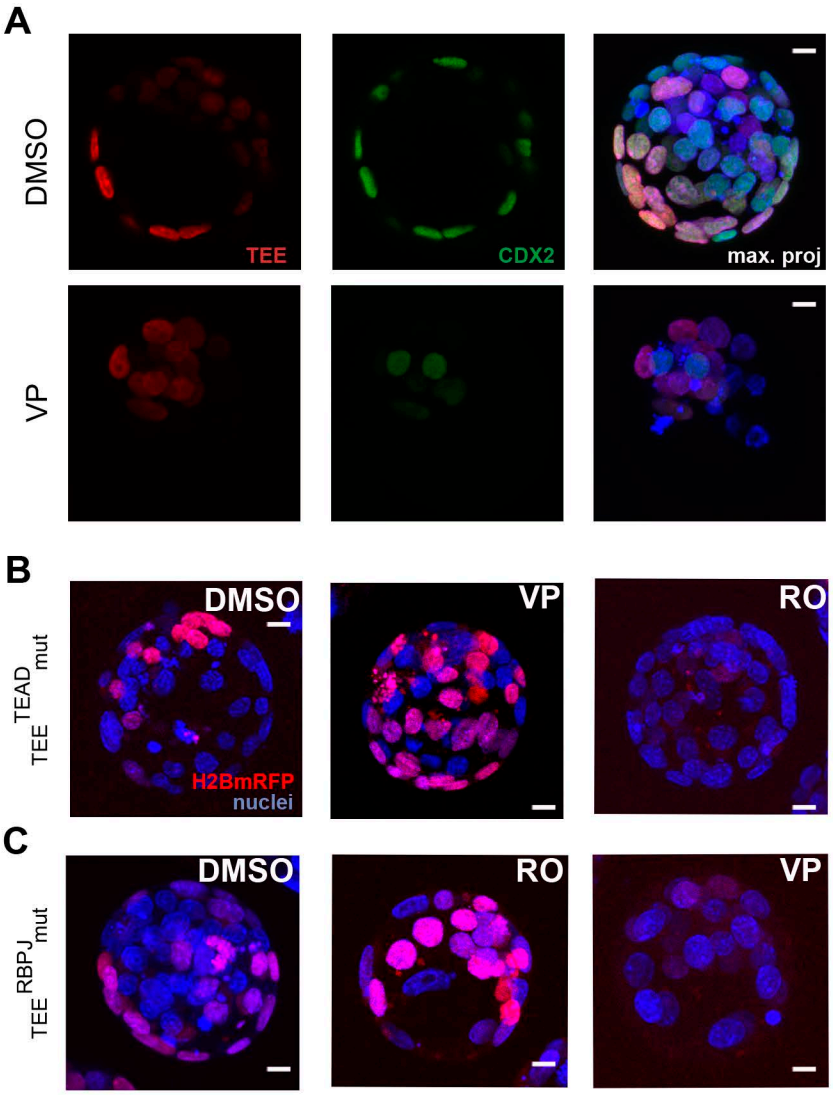
A
DMSO
VP
TEE
CDX2
max. proj
B
TEE TEAD mut
DMSO
VP
RO
H2BmRFP
nuclei
C
TEE RBPJ mut
DMSO
RO
VP

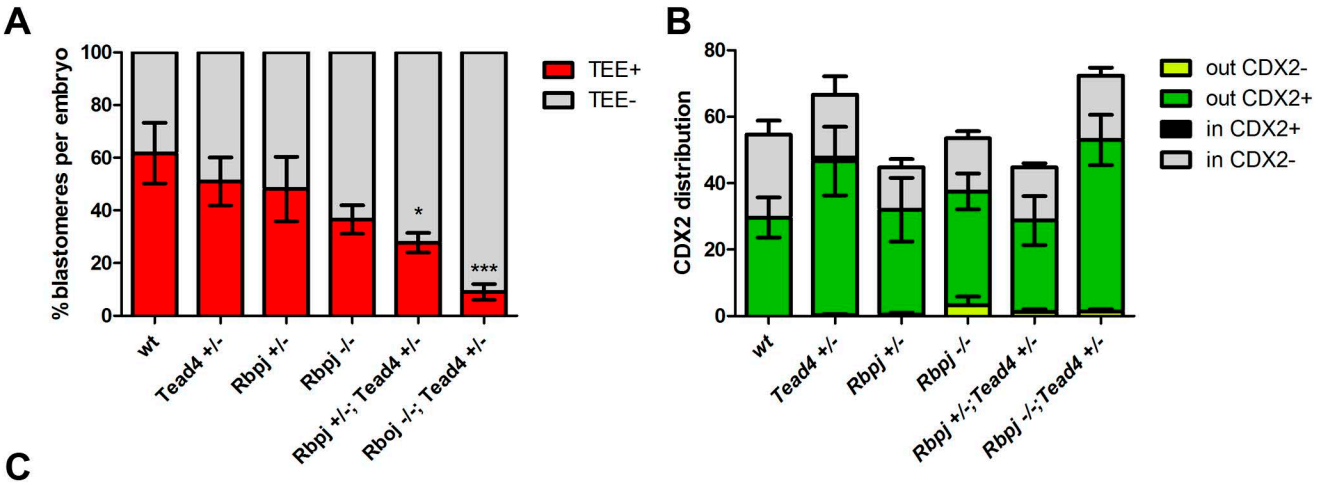

C

Rbpj	+/+	+/+	+/-	+/-	+/+	-/-	+/-	-/-	-/-	
Tead4	+/+	+/-	+/+	+/-	-/-	+/+	-/-	+/-	-/-	total
no. of embryos (%)	13 (16,88%)	10(12,98%)	10 (12,98%)	18(23,37%)	2(2,59%)	7(9,09%)	8(10,39%)	9(11,69%)	0	77
expected %	6,25%	12,50%	12,50%	25,00%	6,25%	6,25%	12,50%	12,50%	6,25%	100,00%

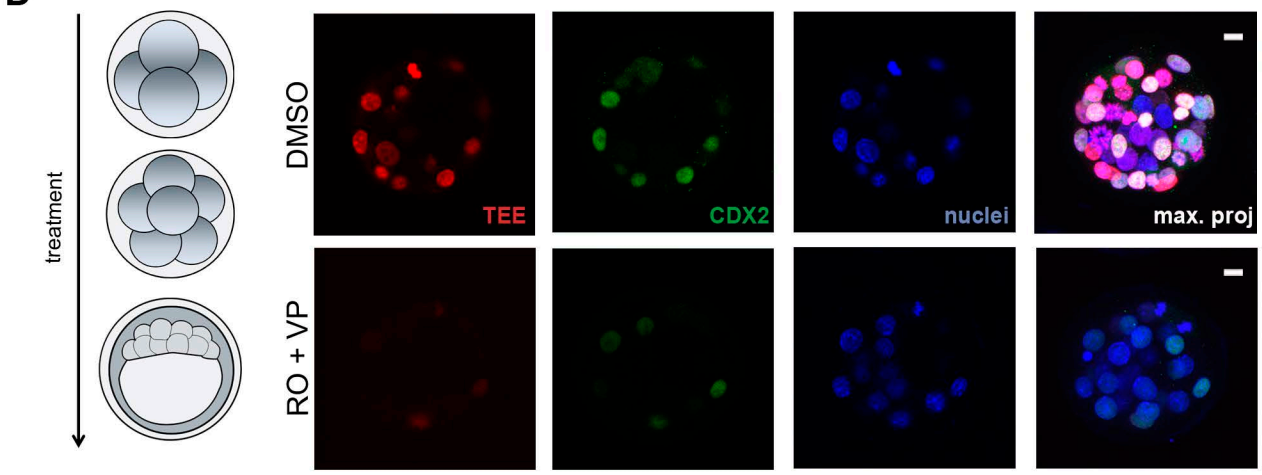

RayonS5

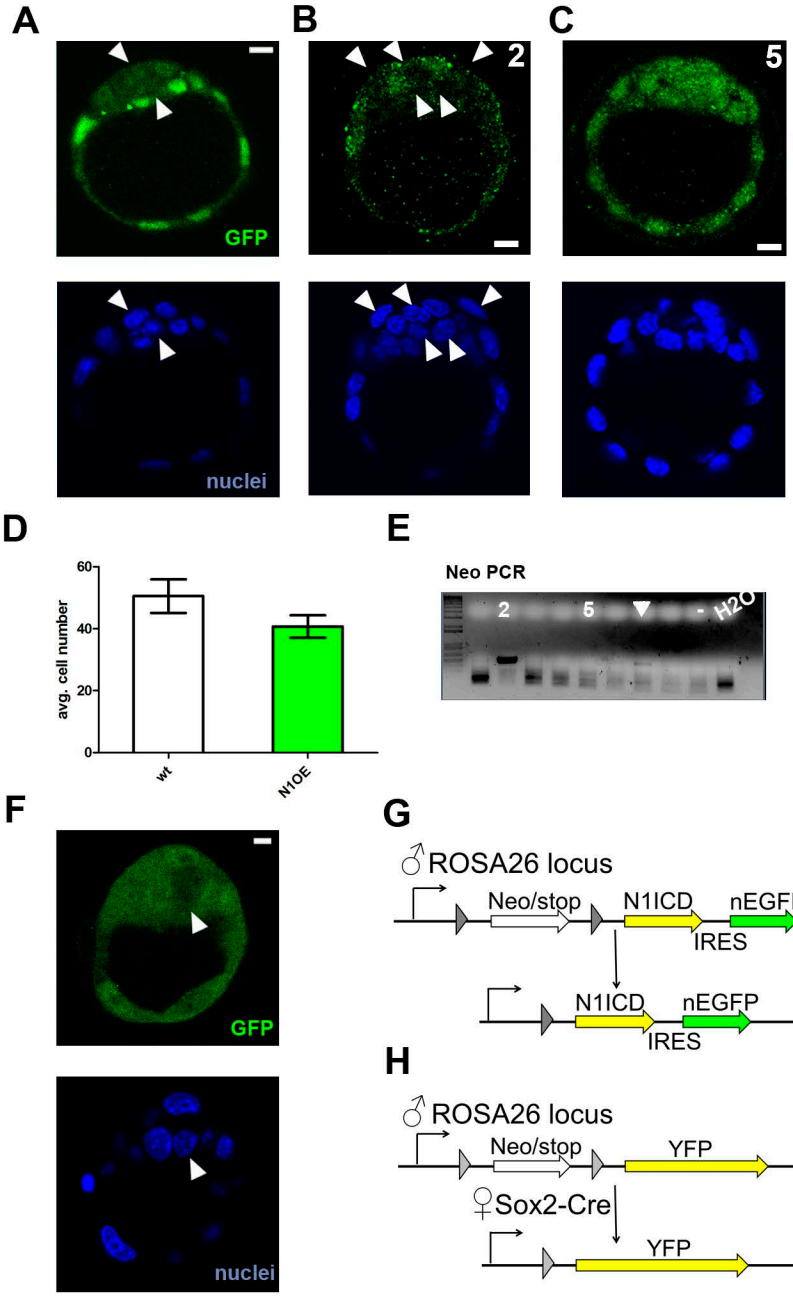
A
B
C
2
5
GFP
nuclei
D
E
avg. cell number
60
40
20
0
wt
N1OE
Neo PCR
2
5
- H2O
F
G
H
GFP
nuclei
♂ROSA26 locus
Neo/stop
N1ICD
nEGFP
IRES
N1ICD
nEGFP
IRES
♂ROSA26 locus
Neo/stop
YFP
♀Sox2-Cre
YFP

RayonS6

SUPPLEMENTAL FIGURE LEGENDS

Figure S1, related to Figure 1: Identification of the *Cdx2* TEE. (A) Diagram of the *Cdx2* locus showing the fragments tested in transient transgenic embryos, the specific activity of the fragments in the TE, and the percentage of embryos for each construct showing any sign of reporter activity. (B) Representative transient transgenic embryos showing *lacZ* reporter activity driven by those constructs showing specific activity in the TE. (C) Temporal dynamics of a stable *lacZ*-TEE line for construct #3 at the 8- and 16-cell and blastocyst stages.

Figure S2, related to Figure 2: The *Cdx2* TEE is not an auto-regulatory element. (A-B) Activity of the TEE, detected by immunohistochemistry with anti-mRFP antibody (red), and immunodetection of CDX2 (green) in (A) wild type (wt) and (B) *Cdx2* mutant blastocysts. Nuclei were stained with DAPI (blue). (C) Average cell number in wild type and *Cdx2* mutant blastocysts (D) Percentage of TEE-positive cells per embryo in wild type (n=149, 4 embryos) and *Cdx2* mutant blastocysts (n=145, 3 embryos). (E) Average cell number in wild type blastocyst, *Tead4* heterozygotes and *Tead4* mutant blastocysts. Differences in cell number between the genotypes is not significant (F) Percentage of TEE-positive cells per embryo in wild type blastocysts (n=218, 3 embryos), *Tead4* heterozygotes (n=464, 8 embryos) and *Tead4* mutant homozygotes (n=78, 2 embryos).

Figure S3, related to Figure 3: Evidence for a role of the Notch signaling pathway in the TE. (A) Sequence of the 1.3 kb TEE, highlighting putative binding sites for RBPJ (blue) and TEAD (green). (B) Immunodetection of N1ICD with the signal enhanced by using a tyramide amplification kit (red). Nuclei were stained with DAPI (blue). Merged image is shown in the right panel. Scale bars, 10 μm.

Figure S4, related to Figure 4: The RBPJ and TEAD binding sites of the TEE are functional. (A) Effect of the TEAD–YAP inhibitor Verteporfin (VP) on TEE activity (red) and endogenous CDX2 (green). (B) TEE^{TEAD}mut activity in transient transgenic embryos treated with DMSO, VP or RO. (C) TEE^{RBPJ}mut activity in transient transgenic embryos treated with DMSO, RO or VP. Nuclei were stained with DAPI. Scale bars, 10 μm.

Figure S5, related to Figure 5: Phenotype of embryos with different *Rbpj*;*Tead4* allelic combinations. (A) Percentage of TEE-positive cells per embryo in wild type blastocysts (n=162, 3 embryos) and in *Tead4*$^{+/-}$ (n=200, 3 embryos), *Rbpj*$^{+/-}$ (n=187, 5 embryos), *Rbpj*$^{-/-}$ (n=115, 3 embryos), *Rbpj*$^{+/-}$*;Tead4*$^{+/-}$ (n=238, 5 embryos) and *Rbpj*$^{-/-}$*;Tead4*$^{+/-}$ allelic combinations (n=176, 2 embryos). *p<0.05, ***p<0.001 by Bonferroni post test. (B) Average number of inside and outside cells positive or negative for CDX2 in *wt* (n=164, 3 embryos), *Tead4*$^{+/-}$ (n=200, 3 embryos), *Rbpj*$^{+/-}$ (n=179, 4 embryos), *Rbpj*$^{-/-}$ (n=214, 4 embryos), *Rbpj*$^{+/-}$*; Tead4*$^{+/-}$ (n=179, 4 embryos) and *Rbpj*$^{-/-}$*;Tead4*$^{+/-}$ allelic combinations (n=217, 3 embryos) quantified in Figure 4F. (C) Distribution (%) of embryos for the different allelic combinations of *Rbpj* and *Tead4*, compared with the expected distribution. Dead embryos inside the zona, which could include double homozygotes, were observed but could not be genotyped due to DNA degradation (Table S1). (D) TEE activity (red) and CDX2 immunodetection (green) in embryos from the mRFP line treated with DMSO or RO+VP from 4 cells until blastocyst stage (left panel). Maximal projections of merged images are shown in the right panels. Nuclei were stained with DAPI. Scale bars, 10 μm.

Figure S6, related to Figure 6: Mosaicism of maternal Sox2-Cre activity in the blastocyst. (A) Mosaicism of reporter expression (green) from the R26-stop-N1ICD-ires-EGFP line when recombined by maternal Sox2-Cre. (B) Example of a blastocyst with a very high proportion of non-recombined cells. (C) Example of a blastocyst with recombination

occurring in all cells. (D) Average cell number in wild type (wt) and N1ICD-overexpressing (N1OE) blastocysts. (E) Detection of mosaic recombination in blastocysts by PCR of Neo. The varying degree of detection of the non-recombined allele in different embryos is shown, ranging from non-recombined (embryo 2, shown in panel B), mosaic recombination (white arrowhead), to full recombination of the Neo allele (embryo 5, shown in panel C). Negative control (-) and H_2O samples are indicated. (F) Reporter mosaicism (cytoplasmic, green) from the R26-stop-YFP line when recombined by maternal Sox2-Cre. (G-H) Breeding strategy for the ♂R26-stop-N1ICD-ires-EGFP X ♀Sox2-Cre cross (G) and for the ♂R26-stop-YFP X ♀Sox2-Cre cross. (H). White arrowheads in (A-C, F) mark non-recombined cells. Nuclei in (A-C and F) were stained with DAPI. Scale bars, 10 μm.